

**NOVEL PROPERTIES AND EMERGENT  
COLLECTIVE PHENOMENA OF ACTIVE FLUIDS**

**A DISSERTATION  
SUBMITTED TO THE FACULTY OF THE GRADUATE SCHOOL  
OF THE UNIVERSITY OF MINNESOTA  
BY**

**ZHENGYANG LIU**

**IN PARTIAL FULFILLMENT OF THE REQUIREMENTS  
FOR THE DEGREE OF  
DOCTOR OF PHILOSOPHY**

**ADVISOR: XIANG CHENG, PH.D.**

**DEC, 2020**

© ZHENGYANG LIU 2020  
ALL RIGHTS RESERVED

# Acknowledgements

# **Dedication**

To my beloved family for supporting me over the years.

## Abstract

An active fluid denotes a suspension of particles, cells and macromolecules that are capable of transducing free energy into systematic motions. Converting energy at individual constituent scales, these systems are constantly driven out of equilibrium and display unusual phenomena, including a transition to a zero viscosity superfluid-like state and a transition to a collective moving turbulent state. These curious transitions are consequences of the self-propulsion of active particles, and are absent in classical complex fluids without spontaneous motions.

In this thesis, we present an experimental investigation on the rheology of active fluids under confinement. Specifically, the viscosity of bacterial suspensions is significantly reduced by confining walls. We show that this effect results from upstream swimming bacteria near the confining walls, which collectively exert stress on the fluids and push the fluids to flow. A phenomenological model is proposed which qualitatively captures the confinement effect on the viscosity of bacterial suspensions.

The collective motions in dense bacterial suspensions are investigated. In particular, we present the first experimental study on the giant number fluctuation - a landmark of collectively moving active particles - in 3-dimensional bacterial suspensions. Our measurements are free from effect of frictional walls and thus allow quantitative comparison with previous theoretical and computational works. We also present a detailed analysis on the flow fields generated by the swimming bacteria, and reveal a strong coupling between flow strength and giant number fluctuations spanning all length scales.

In addition, we measure the critical conditions of the transition from disordered state to turbulent state in bacterial suspensions. We present the experimental results in a phase diagram, serving as a benchmark for existing and future theories. We put forward

a heuristic model based on two-body hydrodynamic interactions, hoping to understand the transition in a more intuitive way and to stimulate theoretical advancement.

By elucidating the causes and consequences these phenomena, we can not only expand the knowledge of active fluids, but also provide deeper understandings on the biological and ecological impact of living organism behavior. Our experiments allow quantitative understanding of active fluids and lay the foundation of applying active fluids to real world challenges.

# Contents

<b>Acknowledgements</b>	<b>i</b>
<b>Dedication</b>	<b>ii</b>
<b>Abstract</b>	<b>iii</b>
<b>List of Figures</b>	<b>vii</b>
<b>1 Experimental Background</b>	<b>1</b>
1.1 Motile Bacteria Sample Preparation . . . . .	2
1.1.1 Background Information . . . . .	3
1.1.2 Protocol . . . . .	5
1.2 Video Microscopy and Image Analysis . . . . .	7
1.2.1 Video Microscopy . . . . .	9
1.2.2 Image Analysis . . . . .	12
1.3 Micro-fabrication and Microfluidic Viscometer . . . . .	18
1.3.1 Micro-fabrication . . . . .	18
1.3.2 Microfluidic Viscometer . . . . .	19
1.4 Light-controlled E. coli: Genetic Modification, Culturing and Trouble Shooting . . . . .	20



# List of Figures

1.1	Figure 2.1:	4
1.2	Figure 2.2:	8
1.3	Figure 2.3:	10
1.4	Figure 2.4:	12
1.5	Figure 2.5:	14
1.6	Figure 2.6:	17
1.7	Microfluidic viscometer fabrication and setup.	19

# Chapter 1

## Experimental Background

In this chapter, experimental techniques that are used in my research will be described briefly as a practical guide for those who want to test or perform some parts of the experiments in this thesis. The following aspects will be covered:

- *Escherichia coli* (*E. coli*) bacterial suspensions are the model throughout the whole thesis, so I will start talking about the preparation of motile bacterial sample in Sec. 1.1.
- Optical microscopy along with digital imaging has been the key approach for investigating the properties of bacterial suspensions. Such approach naturally demands automated image analysis tools. In Sec. 1.2, I will describe in detail some new techniques I have been using that are associated with video microscopy and image analysis.
- When investigating the rheology of bacterial suspensions, we adopted a homemade microfluidic viscometer device. Details of the fabrication are shown in Sec. 1.3.
- A light-powered *E. coli* strain is used in the giant number fluctuations study and the emergence of active turbulence study (Chap. ?? and Chap. ??). This special

strain was obtained by transforming a wild-type strain with an exogenic plasmid which encodes a light-harvesting membrane protein. The discovery and working principles of the light-powering feature has been well documented by earlier works [1, 2, 3, 4, 5]. Following these works, I constructed a plasmid containing the gene and successfully transformed the wild-type *E. coli* strain. In Sec. 1.4, I will present the details on the materials and procedures I used to construct the mutant as a practical guide to those who need to further modify or trouble shoot the strain I made.

## 1.1 Motile Bacteria Sample Preparation

Peritrichous *E. coli* bacteria have been widely used as model micro-swimmers for active fluid studies [6, 7]. By bundling and unbundling their flagella, they achieve a so called “run-and-tumble” motion, allowing them to more efficiently explore their surrounding environment and to search for supplies. Fig. 1.1a shows a simplified model of a swimming *E. coli* bacterium model with a 2  $\mu\text{m}$  rod-shape body and a helical-shape flagellum of around 8  $\mu\text{m}$ . When swimming, all the flagella bundle together behind the cell and propel it forward [8]. Fig. 1.1b-c show the bundled state and unbundled state of the flagella, respectively. A swimming *E. coli* bacterium can generate nontrivial fluid flow, which can lead to hydrodynamic attraction to boundaries, alignment with other bacteria and other consequences [9]. It had long been assumed in theoretical works that the effective flow generated by microswimmers like *E. coli* is dipolar, with one force pushing forward from the head and another force pushing backward from the flagella [10, 11, 12, 13]. This assumption was then experimentally verified by Drescher et al. in 2011 [14], by reconstructing the flow field from many tracer particle trajectories. Fig. 1.1d-e show the flow field they measured and the best-fit force dipole flow. As I will show later, the swimming-induced flow plays a key role in the novel properties and

collective motions in the bacterial active fluids.

There are quite a few research groups over the world that are using *E. coli* suspensions to study active fluids. To name a few, Yodh and Arratia at University of Pennsylvania, Wu at Cornell University, Poon at the University of Edinburgh and Clement at ESPCI all have published experimental works using *E. coli* [16, 17, 18, 19, 20]. Although the protocols of preparing motile *E. coli* samples are similar across different groups' protocols, they have subtle differences from each other, which may be attributed to the specific strain of *E. coli*, ingredients of media and specific instrument conditions. Schwarz-Linek et al. proposed a sample preparation protocol based on standard bio-science manuals [21] and Berg's *E. coli* protocol. If one wants to learn how to prepare motile *E. coli* from scratch, it is recommended to follow the protocol in Ref. [7].

When I joined the Cheng group at the University of Minnesota in 2015, before Ref. [7] was published, there was already a protocol in our lab that worked pretty well for us. I learned the protocol from previous lab members Yi Peng and Devranjan Samanta, and have made some modifications over the years to optimize the motility and concentration of samples and to include the additional procedures for preparing light-powered *E. coli*. Below I describe the protocol that works the best in Cheng lab.

### 1.1.1 Background Information

**Bacterial strains** We primarily work on two *E. coli* strains: *AW804* and *BW25113*.

*AW804* is light-sensitive. *BW25113* is a wild type strain carrying a plasmid encoding green fluorescence protein, thus it is used when fluorescence / confocal microscopy is needed. Both strains have ampicillin resistance marker and thus require supplementing ampicillin to culturing media.

**Antibiotics** Bacteria are ubiquitous in the environment and can easily contaminate our bacterial culture. In order to ensure the fidelity of the culture, we add antibiotic

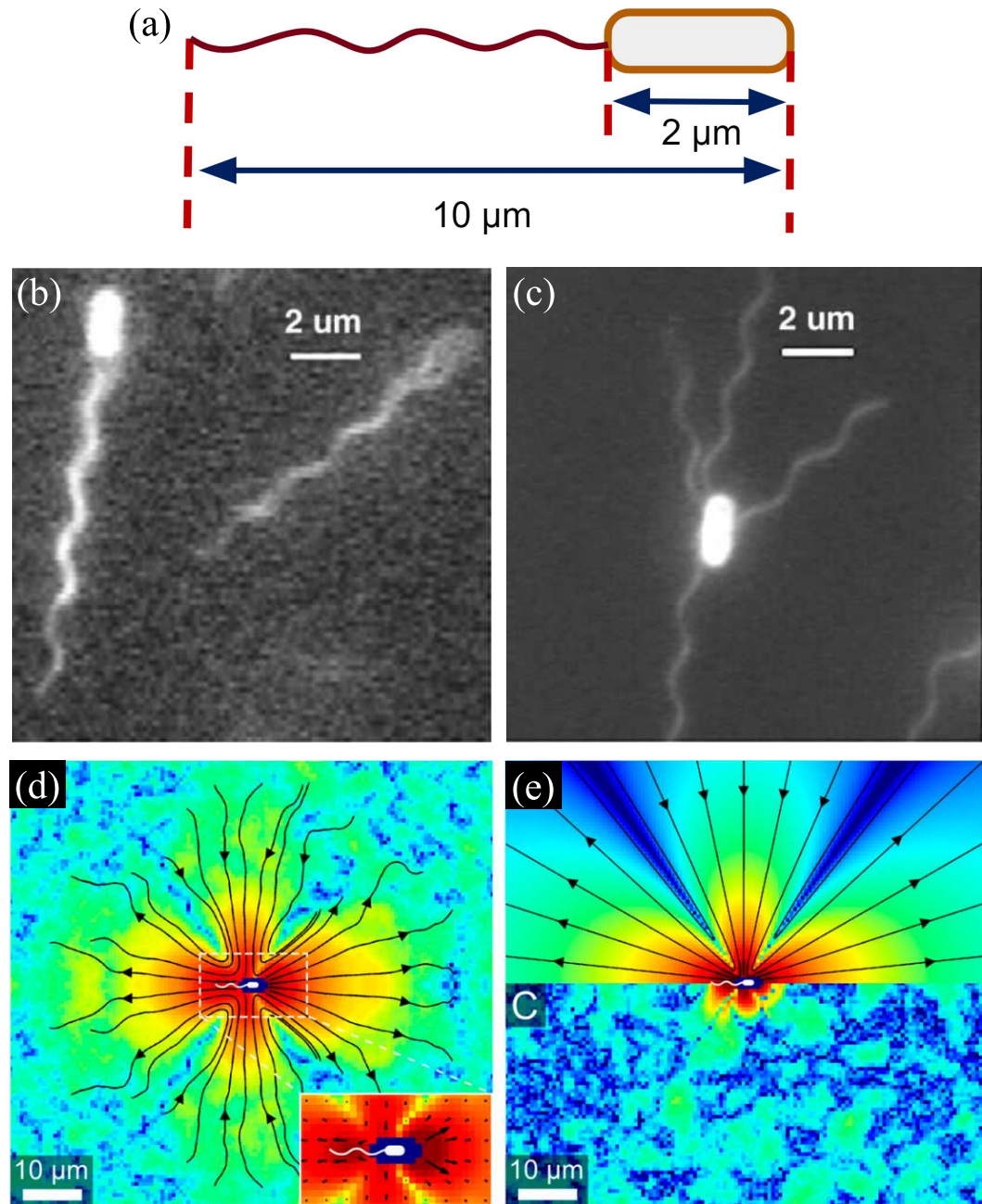


**Figure 1.1: Model swimmer *Escherichia coli* and its flow field.** (a) A schematic of a swimming *E. coli* bacterium. (b) Fluorescence microscopic image of swimming *E. coli* with bundled flagella. (c) Fluorescence microscopic image of tumbling *E. coli* with unbundled flagella. (d) Flow field around a swimming *E. coli*, measured with suspending microspheres. (e) Best-fit force dipole flow for the flow field shown in (d). Image sources: (b) and (c) are reproduced from Fig. 4a and 2a in Ref. [15] with permission from XXX. (d) and (e) are reproduced from Fig. 1a and 1b in Ref. [14] with permission from XXX.

resistance markers to the bacteria we want to grow and meanwhile add antibiotics to the medium. The antibiotics inhibit the growth of contaminating species and allow our desired bacteria to grow normally.

**Medium** Various types of media (terrific broth, Luria broth, 2XYT and M9, etc.) are commonly used for bacterial culture. We use terrific broth. The recipe can be found in the protocol section.

### 1.1.2 Protocol

1. Prepare a 2-ml *E. coli* overnight culture.

(a) Prepare liquid terrific broth (TB). For example, to make 1 L TB, weigh out the following into a 1 L glass bottle:

- 23.6 g Yeast extract (Sigma-Aldrich)
- 11.8 g Tryptone plus (Sigma-Aldrich)
- 4 ml Glycerol (XXX)
- Add dI water to 1 L

Loosely close the cap on the bottle (do NOT close all the way or the bottle may explode!) and then loosely cover the top of the bottle with autoclave tape (stick cap and bottle body together to avoid cap popping off). Autoclave and allow to cool to room temperature. Now screw on the top of the bottle and store the TB at room temperature.

- (b) Using a sterile 10 ml pipette, transfer 2 ml TB to a sterile glass test tube.
- (c) Using a sterile pipette, add 2 microliter (0.1% v/v) antibiotic solution to the TB in test tube.

- (d) Using a sterile pipette tip, pick a small chunk from our bacterial frozen stock (stored in the -80 °C freezer in 251) and carefully transfer the small chunk into the liquid TB + antibiotic.
- (e) Loosely cover the culture with sterile cap that is not air tight.
- (f) Incubate bacterial culture at 37 °C for 12-18 h in a shaking incubator.
- (g) After incubation, check growth, which is characterized by a cloudy haze in the media. This is the overnight culture.
2. Dilute overnight culture and harvest motile bacteria at mid-late log phase.
- (a) Using a sterile 10 ml pipette, transfer 3 ml TB to a sterile glass test tube.
- (b) Using a sterile pipette, add 2 microliter (0.1% v/v) antibiotic solution to the TB in test tube.
- (c) Transfer 30 microliter (1% v/v) overnight culture into the liquid TB + antibiotic.
- (d) Incubate bacterial culture at 30 °C for 6-6.5 h in a shaking incubator.
- (e) After incubation, check for growth, which is characterized by a cloudy haze in the media. This is the log phase bacteria.
3. Centrifuge for better motility and higher concentration bacterial sample.
- (a) Prepare motility buffer (MB), the following recipe is from Ref. [22].
- 0.01 M potassium phosphate (combine monobasic and dibasic solutions, Sigma-Aldrich)
  - $10^{-4}$  M EDTA (Sigma-Aldrich)
  - 0.002% weight fraction Tween 20 (Sigma-Aldrich)
  - Adjust pH to 7.0

- (b) Take out the log phase bacteria from the shaking incubator, centrifuge for 5 min at 800 rcf.
- (c) Discard the supernatant quickly and transfer the left-over liquid to a new centrifuge tube.
- (d) Add 500-1000 ul MB (or water) to resuspend the bottom pellet (avoid bottom pellet) and centrifuge for a second time (5 min, 800 rcf).
- (e) Discard the supernatant and let the tubes sit for two minutes. The remaining left-over liquid should be now filled with the active *E. coli*. Take the left-over solution in another capsule and use it for experiments.
- (f) To measure the concentration, transfer 10 microliter of the suspension into a 1 ml plastic cuvette and dilute 100 times (by adding 990 microliter water). Put the cuvette in the spectrophotometer in 251 and use the OD600 program. The resulting number times 100 will be the number density of your suspension in the unit of  $n_0$  ( $8 \times 10^8$  cells/ml).

## 1.2 Video Microscopy and Image Analysis

In my experimental research, a standard workflow is

- Take videos of samples such as swimming bacteria
- Analyze the videos, typically extracting particle position and velocity information from the videos
- Calculate from the position and velocity information to obtain more complex information, such as flow field, kinetic energy and diffusivity

From this workflow, one can tell that the video microscopy and image analysis are the core skills that enable me to conduct the research. In this section, I will decribe how I

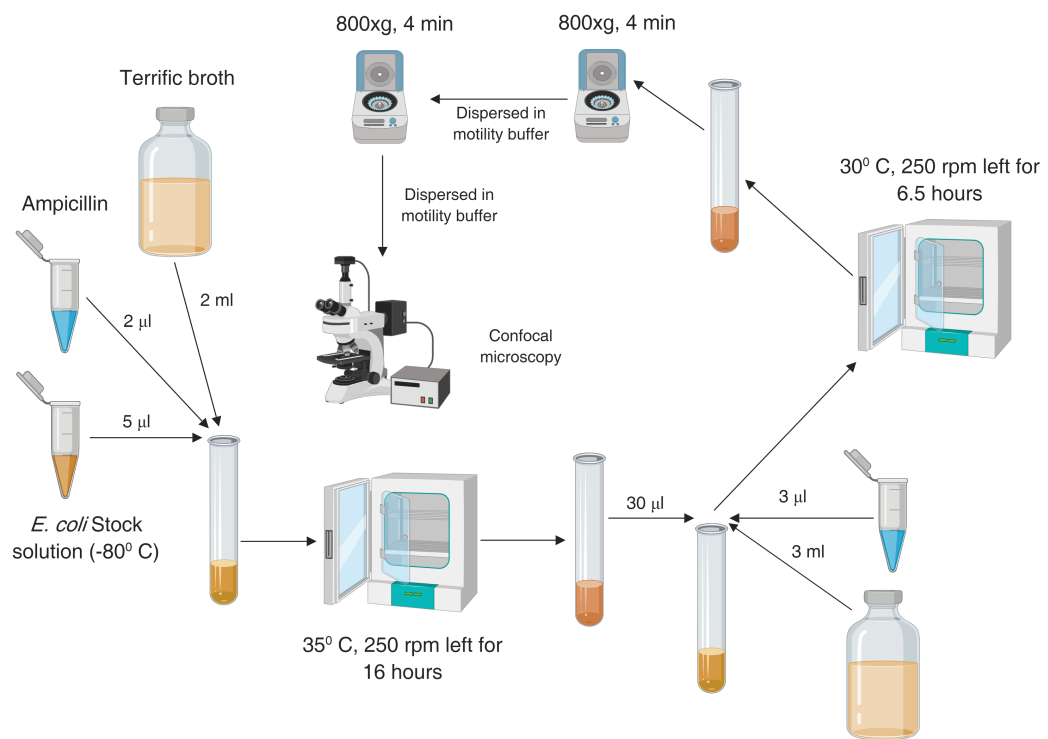


Figure 1.2: **Graphical motile *E. coli* sample preparation protocol.** Image courtesy of Shashank Kamdar.

overcome practical challenges when applying these skills in experiments. I want to note that the standard manuals are always the best reference for beginners who have just started to learn about a technique. In my case, the standard manuals are the Nikon inverted microscope Eclipse Ti-E/Ti-E/B instructions [23], OpenPIV official website [24, 25] and trackpy official website [26]. Some related projects (listed in the websites mentioned) also provide valuable tutorials and ideas, for example the particle tracking routines in IDL by Crocker and Weeks [27] and in Matlab by Blair and Dufresne [28].

### 1.2.1 Video Microscopy

#### Power *E. coli* with Illumination Light

In the studies of the giant number fluctuations and the emergence of active turbulence, I used a light-powered *E. coli* mutant, which changes its swimming speed according to the amount of light it receives (details of the light-powered *E. coli* mutant can be found in Sec. 1.4).

I use the illumination light of the microscope as the power source of the bacteria, instead of using another light source, based on two considerations: 1) an additional light source shining on the sample will lead to additional unexpected light going into the objective, which often leads to bad image quality; 2) It is hard to construct a spatially uniform light, especially when it has to come in an angle not perpendicular to the specimen. Therefore, I use the illumination light of the microscope to power the *E. coli*.

The light-powered *E. coli* mutant requires quite a high light intensity to move fast enough. Such a high intensity cannot be achieved in the normal microscopy conditions, where four light filters are applied for different purposes. Fig. 1.3a-b show the Nikon Ti-E inverted microscope and the illumination light filtering system with the four light filters designated as ND, D, NCB and PFS. The functions of the filters are listed in

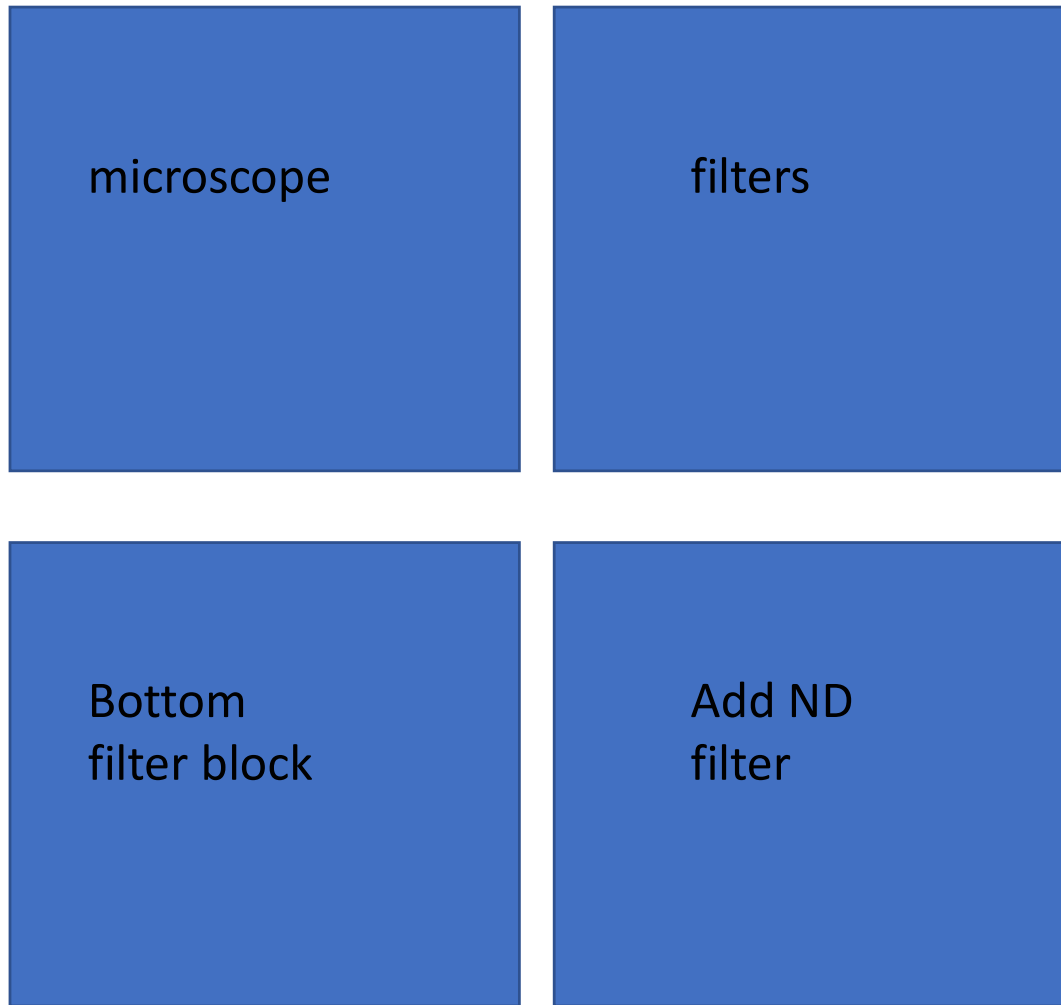


Figure 1.3: **Nikon Ti-E inverted microscope and its filters.** (a) Nikon Ti-E inverted microscope model. (b) Illumination light path filters. (c) Filter block under objective. (d) Adding additional ND filter under objective.

Table. 1.1:

<b>ND</b>	Neutral density filter: adjust the brightness for normal microscopy or photomicroscopy
<b>D</b>	Diffusion filter: made of frosted glass and will diffuse light, used for equalizing the illumination
<b>NCB</b>	Neutral color balance: corrects the color temperature for mnormal microscopy or filming by daylight type color. Note: this filter is essential for optimal color reproducibility when taking color images, and it should be kept out of the optical path when filming in black and white.
<b>PFS</b>	Perfect focusing system: a hardware solution to combat axial focus fluctuations in real time during long-term imaging investigations. Note - this filter should be kept out if one does not intend to use the perfect focusing system.

Table 1.1: Filters in the illumination light path and their functions.

Removing some of those filters can make the illumination light strong enough to power the bacteria. According to the functions of the filters, the only necessary filter is the diffusion filter, given that one is not doing color imaging and is not using perfect focusing system, as it is in my experiment. Fig. 1.4a shows an image taken without the diffusion filter (D). Without diffusing the illumination light, the resulting image is clearly inhomogeneous in a large range, with a bright center and a dark bottom area. By putting the diffusion filter in the illumination light path, one can make the illumination light much more uniform, as shown in Fig. 1.4b. All the other filters (ND, NCB, PFS) are effectively reducing the overall intensity. Putting in or out these filters only results in globally dimmer or brighter images, without changing the detailed patterns in the image. Thus, these three filters are optional in my experiment. Since powering the light-powered *E. coli* requires a very high light intensity, only the diffusion filter should be kept in the illumination light path.

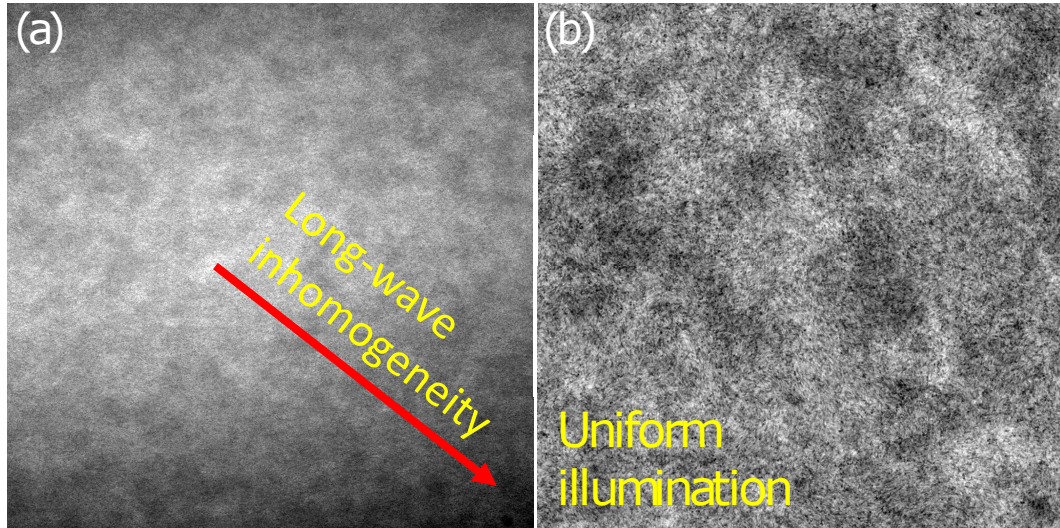


Figure 1.4: Image with (a) and without (b) the diffusion filter (D).

### Avoid over exposure

While I have achieved high enough light intensity to power the bacteria, another problem occurs - the light is so strong that the camera is over exposed. In order to power the bacteria, the illumination light intensity cannot be reduced. The only way to avoid the over exposure is to add an filter between the specimen and the camera. What I did is shown in Fig. 1.3c-d. I took out one of the filter cube from the turret under the objective, which is originally used for fluorescence microscopy. Then I put a piece of neutral density filter on top of the cube and put the cube back to the turret. This additional filter allows for the imaging under strong illumination light.

### 1.2.2 Image Analysis

With the fast developments of digital imaging, human are enabled to investigate many processes, ranging from astronomical object motions to microorganism behavior, in unprecedented detail [29]. While it is getting easier than ever to acquire large amount

of images, a demand for automated image analysis has also become unprecedented [30, 31, 32].

Particle tracking has been one of the most useful automated image analysis tools in the study of colloids and microorganisms. Over the last 20 years, it has developed significantly and many algorithms, toolkits and all-in-one softwares have been implemented and applied in a variety of image analysis tasks. Despite the abundance of particle tracking tools, no agreement has been made on which one in the vast collection of tools works best. Much effort has been devoted to answer this question by comparing the performance of different tools [29, 33, 34, 35, 36, 37, 38, 39]. In these studies, though different algorithms show different performance, no single algorithm outperforms all the others in all scenarios.

Particle tracking is generally composed of two steps: particle detection (spatial) and linking trajectories (temporal). For the detection step, based on the feature (generalized “particle”) shape sought, different methods are used. For point features, a local maxima finding method is often used; for edge features, group labeling is often used; and for region features, region seeding is often used [33].

### Anisotropic Particle Tracking

A challenge I encountered when working on the diffusion project was the detecting of the ellipsoidal particles surrounded by moving microorganisms (bacteria and algae). A local maxima finding method was applied previously to detect the center of an ellipsoidal particle [40]. Combined with intensity fitting around the center in different directions, the orientation of the particle can also be obtained. The same method, however, does not work well for my image because of the presence of microorganisms, which give rise to many more local maxima in the image (a typical image is shown in Fig. 1.5a). To overcome this challenge, I adapted a thresholding and connected group labeling based

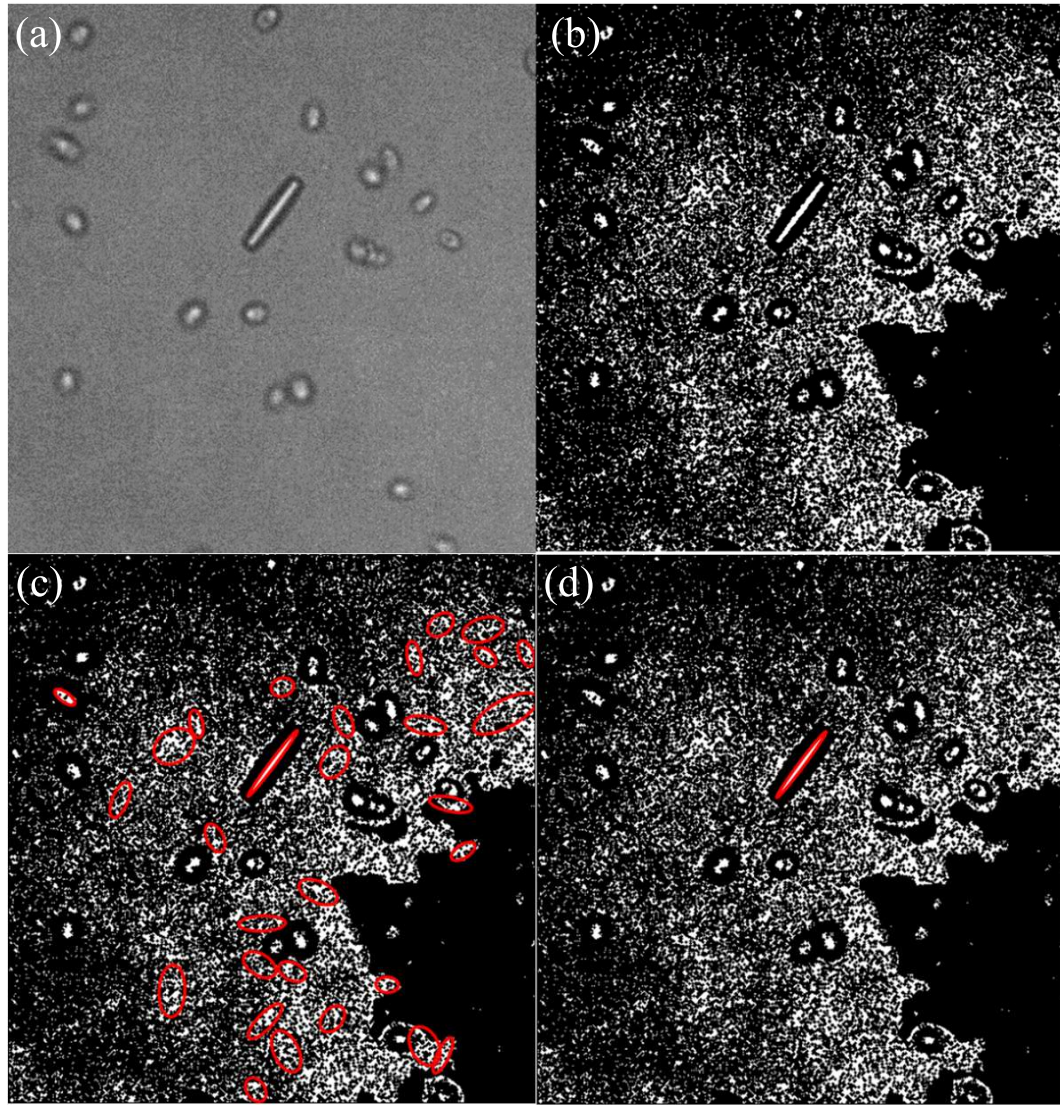


**Figure 1.5: Illustration of ellipsoidal particle detection by thresholding and group labeling.** (a) The raw image: an ellipsoidal polystyrene particle surrounded by swimming algae in a suspension. (b) Binarized raw image. (c) Detection result of connected white regions. (d) Final result after appropriate filtering.

method from Ref. [41, 42, 43]. The method has the following steps:

- threshold the grayscale image (Fig. 1.5a) to a binary image (Fig. 1.5b)

- find connected white regions (`skimage.measure.label` in Python)
- find the best-fit ellipse of each white connected regions found in the last step, as indicated by the red ellipses in Fig. 1.5c (`skimage.measure.regionprops` in Python)
- filter the parameters of the ellipses with appropriate criteria, so that only the desired ellipse is found, as indicated by the red ellipse in Fig. 1.5d

Fig. 1.5 only illustrates the essential idea of the method. When applying the method, some necessary image preprocessing, including linear, nonlinear and frequency filters need to be used to make sure the desired features stand out, and the undesired noises are suppressed. The preprocessing techniques have been reviewed in Ref. [33, 32]. This method was used to obtain the trajectories of ellipsoidal particles in algal suspensions, which was then used to calculate the diffusivity for my first collaborative project, reported in Ref. [44].

### **Manual Particle Tracking Software: *manTrack***

Despite the great advances of particle tracking techniques, the accuracy suffers much from poor image quality and mutual touching of objects in images, especially when imaging dense suspensions of microorganisms [34]. A very challenging particle detecting task is manifested by a dense suspension of collectively moving bacteria, as shown in Fig. 1.6a. Despite the use of confocal microscopy, most bacteria are seen to be overlapping with others and are in very different shapes, making it impossible for existing tools to detect all the desired features. In a scenario like this, human eyes are the most powerful complementary tool to machines.

Manually marking the positions of particles is feasible when one image only contains one or several particles. When particle numbers get large, however, it is no longer

feasible (a typical video I take contains hundreds of particles). I combined the automated tracking and the manual tracking together in order to take the advantages of both: fast and reliable, by implementing a manual tracking software *manTrack* with graphical user interface (GUI). The workflow for using *manTrack* is:

- Use an automated method to do a preliminary particle tracking (or detection).
- Load the preliminary automated detection result into *manTrack*. The result will be displayed in *manTrack* GUI as elliptical contours, as shown in Fig. 1.6b.
- When “delete mode” is enabled, one can delete one entry from the result by clicking on the elliptical contour. In Fig. 1.6c, the entry at the tip of the red arrow has been deleted.
- When “track mode” is enabled, one can add an entry to the current result by drawing an ellipse in the image, as shown by the black contour in Fig. 1.6d.

*manTrack* provides a user friendly GUI for efficient modification of preliminary automated particle detection results. The combination of machine automated detection and human eye detection makes possible good accuracy and an acceptable execution speed. This software was used for analyzing the orientation of bacteria in active turbulence (Chap. ??).

Several new tools have been developed in recent years, such as *TrackMate* and *tTt* [45, 39]. The fast growth of technologies in other fields, especially artificial intelligence, has stimulate the development of new tracking techniques [46, 47].

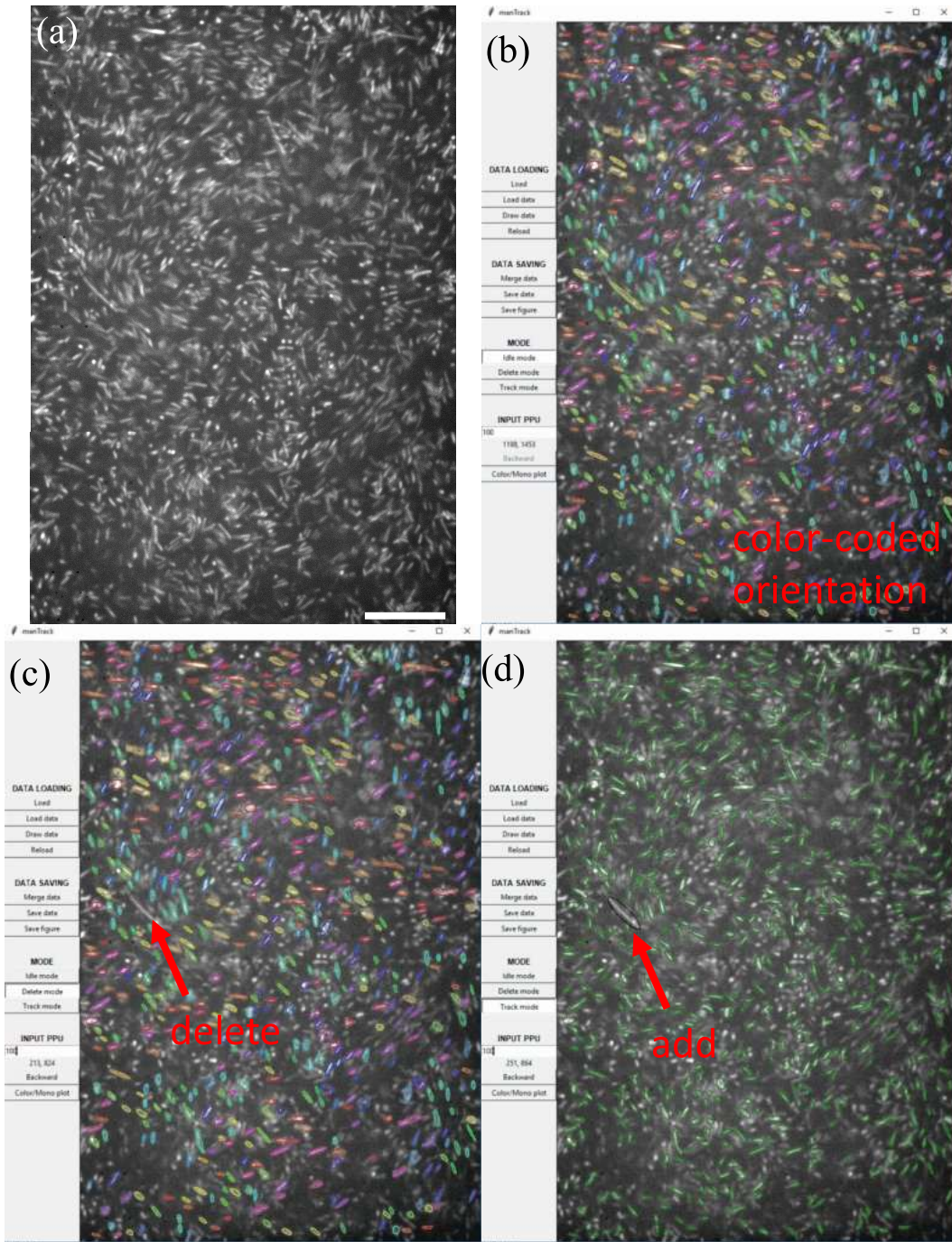


Figure 1.6: **A challenging particle detection task and the manual tracking software.** (a) Confocal microscopy image of *E. coli* collective motion ( $\phi = 6.4\%$ ). (b)-(d) Snapshots of the manTrack software, demonstrating color-coded orientation, manual deleting and manual adding.

## 1.3 Micro-fabrication and Microfluidic Viscometer

### 1.3.1 Micro-fabrication

We used a standard micro-fabrication technique, soft lithography, to produce the microfluidic viscometer we used in the rheology project (Chap. ??) [48]. Such a fabrication usually involves the following steps: experimental design, pattern design, mask fabrication, master fabrication and elastomeric stamp fabrication. After deciding on using the Y-shaped channel viscometer (Fig. 1.7a) [49], I did the pattern design and the staff at Minnesota Nano Center (MNC) had the mask fabricated for me. With the mask, I fabricated the masters of the Y-shaped channel viscometer for various channel heights using the MNC facilities. Then the masters were used for fabricating elastomeric stamps, using Sylgard 184 Silicone Elastomer Kit (Dow Inc.).

To produce masters for the various channel heights, different photoresists need to be used. I chose the SU-8 3000 series photoresists due to their good adhesion property and reduced coating stress, as well as their ready availability in the MNC labs. SU-8 3025 was used for channel heights from 25 to 50  $\mu\text{m}$ . SU-8 3050 was used for channel heights from 50 to 128  $\mu\text{m}$ . Following the procedures described in the photoresist manual, which includes substrate preparation, spin coating, soft bake, exposure, post exposure bake and develop, a photoresist patterned silicon wafer can be produced (Fig. 1.7b).

The elastomeric stamp is fabricated by pouring the Sylgard 184 Silicone Elastomer Kit, which contains a base and a crosslinker in a volume ratio 10:1, onto the photoresist masters. After curing for 3 hours at 70 °C, the pattern of the master mold was perfectly replicated on the solidified elastomer. Finally, a piece of coverslip was stuck on the patterned side of the elastomer by plasma cleaning the surfaces of both. The microfluidic channel is shown in Fig. 1.7c. The length and width of the two arms are 1 cm and 300  $\mu\text{m}$ , respectively. The length and width of the main channel are 4 cm and 600  $\mu\text{m}$ ,

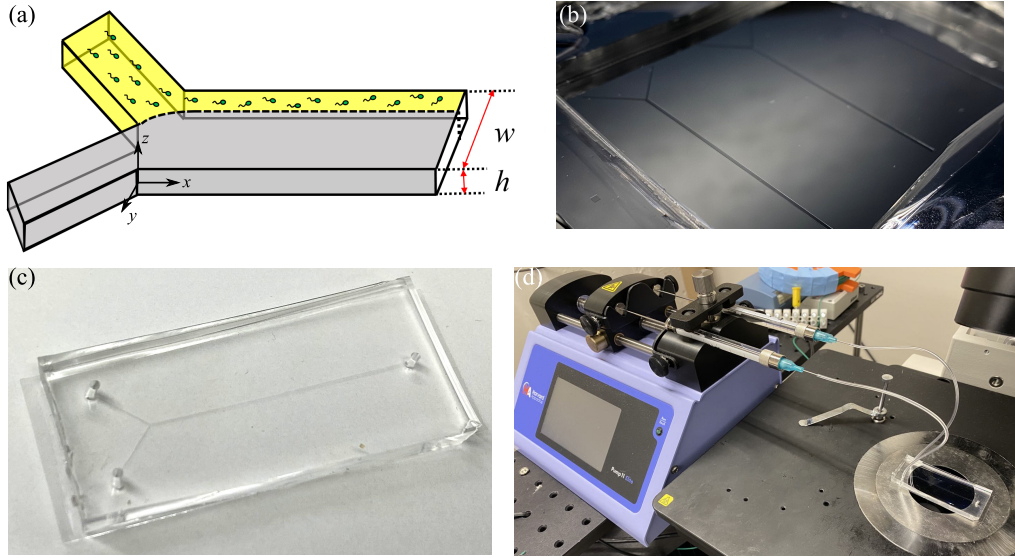


**Figure 1.7: Microfluidic viscometer fabrication and setup.** (a) A sketch of the Y-shaped channel microfluidic viscometer. (b) Master mold of the channel. (c) PDMS Y-shaped channel microfluidic viscometer. (d) Viscometer connected to a syringe pump by plastic tubes, placed on Nikon inverted microscope specimen stage.

respectively. The height of the channel  $h$  ranges from  $25 \mu\text{m}$  to  $128 \mu\text{m}$ . Two cylindrical holes were punched at the ends of the two arms so that fluids can be pumped in.

### 1.3.2 Microfluidic Viscometer

To use the microfluidic viscometer, we connected it with a precision syringe pump (Harvard Apparatus, Elite 11) through elastic tubes, as shown in Fig. 1.7. The two syringes contained two different fluids: one was the bacterial suspension with viscosity to be measured, and the other was a reference fluid with known viscosity, typically water. The two fluids were pumped into the viscometer at the same volumetric flow rate  $Q$ .

The working principle of the viscometer is based on an idea that thicker fluids flow slower than thinner ones. More formally, if we examine a fluid with viscosity  $\eta$ , driven by

a pressure gradient  $\frac{dp}{dx}$  to flow in the  $x$  direction between two parallel no-slip boundaries at  $z = \pm \frac{h}{2}$ , as shown in Fig. 1.7a. At low  $Re$  limit, the flow rate regime of interest, the flow is governed by Navier-Stokes equation

$$0 = -\frac{dP}{dx} + \eta \frac{d^2 u_x}{dz^2} \quad (1.1)$$

The resulting flow is parabolic in  $x$ - $z$  plane and is approximately constant in  $y$ -direction, and can be described by Eq. 1.2

$$u_x(z) = \frac{1}{2\eta} \frac{dP}{dx} \left( \frac{y^2}{h^2} - \frac{1}{4} \right) \quad (1.2)$$

For two different fluids with viscosities  $\eta_1$  and  $\eta_2$ , the mean flow velocity in  $x$ -direction  $\langle u_1 \rangle$  and  $\langle u_2 \rangle$  are related to each other by

$$\frac{\langle u_1 \rangle}{\langle u_2 \rangle} = \frac{\eta_2}{\eta_1} \quad (1.3)$$

noting that the flow rate  $Q = \langle u \rangle dh$ , where  $d$  is the width ( $y$ -direction) of the flow, we can substitute the velocities  $\langle u_1 \rangle$  and  $\langle u_2 \rangle$  in Eq. 1.3 to get

$$\frac{d_1}{d_2} = \frac{\eta_1}{\eta_2} \quad (1.4)$$

Eq. 1.4 is the working equation of the microfluidic viscometer. By imaging and measuring the width  $d_1$  and  $d_2$  of the two fluids in the channel, and combining the known viscosity of the reference fluid  $\eta_2$ , we can measure  $\eta_1$ .

## 1.4 Light-controlled E. coli: Genetic Modification, Culturing and Trouble Shooting

# Bibliography

- [1] O. Beja, L. Aravind, E. V. Koonin, M. T. Suzuki, A. Hadd, L. P. Nguyen, S. B. Jovanovich, C. M. Gates, R. A. Feldman, J. L. Spudich, E. N. Spudich, and E. F. DeLong. Bacterial rhodopsin: Evidence for a new type of phototrophy in the sea. *Science*, 289(5486):1902–1906, 2000.
- [2] Sriram Subramanlam and Richard Henderson. Molecular mechanism of vectorial proton translocation by bacteriorhodopsin. *Nature*, 406(6796):653–657, 2000, NIHMS150003.
- [3] José R. De la Torre, Lynne M. Christianson, Oded Béjà, Marcelino T. Suzuki, David M. Karl, John Heidelberg, and Edward F. DeLong. Proteorhodopsin genes are distributed among divergent marine bacterial taxa. *Proceedings of the National Academy of Sciences of the United States of America*, 100(22):12830–12835, 2003.
- [4] Jessica M. Walter, Derek Greenfield, Carlos Bustamante, and Jan Liphardt. Light-powering *Escherichia coli* with proteorhodopsin. *Proceedings of the National Academy of Sciences of the United States of America*, 104(7):2408–2412, 2007.
- [5] Nico J. Claassens, Michael Volpers, Vitor A.P.Martins dos Santos, John Van der Oost, and Willem M. de Vos. Potential of proton-pumping rhodopsins: Engineering photosystems into microorganisms. *Trends in Biotechnology*, 31(11):633–642, 2013.

- [6] W. C.K. Poon. From Clarkia to escherichia and janus: The physics of natural and synthetic active colloids. *Proceedings of the International School of Physics "Enrico Fermi"*, 184:317–386, 2012, 1306.4799.
- [7] Jana Schwarz-Linek, Jochen Arlt, Alys Jepson, Angela Dawson, Teun Vissers, Dario Miroli, Teuta Pilizota, Vincent A. Martinez, and Wilson C.K. Poon. Escherichia coli as a model active colloid: A practical introduction. *Colloids and Surfaces B: Biointerfaces*, 137:2–16, 2016, 1506.04562.
- [8] Eric Lauga. Bacterial Hydrodynamics. *Annual Review of Fluid Mechanics*, 48:105–130, 2016, 1509.02184.
- [9] J. Elgeti, R. G. Winkler, and G. Gompper. Physics of microswimmers - Single particle motion and collective behavior: A review. *Reports on Progress in Physics*, 78(5), 2015, 1412.2692.
- [10] Aditi R. Simha and Sriram Ramaswamy. Hydrodynamic fluctuations and instabilities in ordered suspensions of self-propelled particles. *Physical review letters*, 89(5):058101, 2002, 0108301.
- [11] Takuji Ishikawa and T. J. Pedley. The rheology of a semi-dilute suspension of swimming model micro-organisms. *Journal of Fluid Mechanics*, 588:399–435, 2007.
- [12] David Saintillan and Michael J. Shelley. Instabilities and pattern formation in active particle suspensions: Kinetic theory and continuum simulations. *Physical Review Letters*, 100(17):1–4, 2008.
- [13] David Saintillan and Michael J. Shelley. Instabilities, pattern formation, and mixing in active suspensions. *Physics of Fluids*, 20(12), 2008.

- [14] Knut Drescher, Jörn Dunkel, Luis H. Cisneros, Sujoy Ganguly, and Raymond E. Goldstein. Fluid dynamics and noise in bacterial cell-cell and cell-surface scattering. *Proceedings of the National Academy of Sciences of the United States of America*, 108(27):10940–10945, 2011.
- [15] Linda Turner, William S. Ryu, and Howard C. Berg. Real-time imaging of fluorescent flagellar filaments. *Journal of Bacteriology*, 182(10):2793–2801, 2000.
- [16] D. T.N. Chen, A. W.C. Lau, L. A. Hough, M. F. Islam, M. Goulian, T. C. Lubensky, and A. G. Yodh. Fluctuations and rheology in active bacterial suspensions. *Physical Review Letters*, 99(14):1–4, 2007, 0709.1465.
- [17] Alison E. Patteson, Arvind Gopinath, Prashant K. Purohit, and Paulo E. Arratia. Particle diffusion in active fluids is non-monotonic in size. *Soft Matter*, 12(8):2365–2372, 2016, 1505.05803.
- [18] T. V. Kasyap, Donald L. Koch, and Mingming Wu. Hydrodynamic tracer diffusion in suspensions of swimming bacteria. *Physics of Fluids*, 26(8), 2014.
- [19] Alys Jepson, Vincent A. Martinez, Jana Schwarz-Linek, Alexander Morozov, and Wilson C.K. Poon. Enhanced diffusion of nonswimmers in a three-dimensional bath of motile bacteria. *Physical Review E - Statistical, Nonlinear, and Soft Matter Physics*, 88(4):3–7, 2013, 1307.1274.
- [20] Gastón Miño, Thomas E. Mallouk, Thierry Darnige, Mauricio Hoyos, Jeremi Dauchet, Jocelyn Dunstan, Rodrigo Soto, Yang Wang, Annie Rousselet, and Eric Clement. Enhanced diffusion due to active swimmers at a solid surface. *Physical Review Letters*, 106(4):1–4, 2011, 1012.4624.
- [21] Alan J. Hargreaves Philip L.R. Bonner. *Basic Bioscience Laboratory Techniques: A Pocket Guide*. 2011.

- [22] Yi Peng, Lipeng Lai, Yi Shu Tai, Kechun Zhang, Xinliang Xu, and Xiang Cheng. Diffusion of ellipsoids in bacterial suspensions. *Physical Review Letters*, 116(6):1–5, 2016, 1509.05893.
- [23] Nikon Instruments Inc. Nikon inverted microscope eclipse ti-e ti-e/b instructions: <http://squishycell.uchicago.edu/manuals/ti-e>
- [24] Z. J. Taylor, R. Gurka, G. A. Kopp, and A. Liberzon. Openpiv official website: <http://www.openpiv.net/>.
- [25] Z. J. Taylor, R. Gurka, G. A. Kopp, and A. Liberzon. Long-duration time-resolved piv to study unsteady aerodynamics. *IEEE Transactions on Instrumentation and Measurement*, 59(12):3262–3269, 2010.
- [26] Casper van der Wel, Daniel Allan, Nathan Keim, and Thomas Caswell. trackpy official website: <http://soft-matter.github.io/trackpy/v0.4.2/>.
- [27] John C. Crocker and Eric R. Weeks. Particle tracking using idl: <http://www.physics.emory.edu/faculty/weeks//idl/index.html>.
- [28] Daniel Blair and Eric Dufresne. The matlab particle tracking code repository: <http://site.physics.georgetown.edu/matlab/>.
- [29] Yannis Kalaidzidis. Intracellular objects tracking. *European Journal of Cell Biology*, 86(9):569–578, 2007.
- [30] Erik Meijering, Ihor Smal, and Gaudenz Danuser. Tracking in molecular bioimaging. *IEEE Signal Processing Magazine*, 23(3):46–53, 2006.
- [31] Khuloud Jaqaman, Dinah Loerke, Marcel Mettlen, Hirotaka Kuwata, Sergio Grinstein, Sandra L. Schmid, and Gaudenz Danuser. Robust single-particle tracking in live-cell time-lapse sequences. *Nature Methods*, 5(8):695–702, 2008.

- [32] Karl Rohr, William J. Godinez, Nathalie Harder, Stefan Wörz, Julian Mattes, Wolfgang Tvarusko, and Roland Eils. Tracking and quantitative analysis of dynamic movements of cells and particles. *Cold Spring Harbor Protocols*, 5(6):1–17, 2010.
- [33] Jonas F. Dorn, Gaudenz Danuser, and Ge Yang. Computational Processing and Analysis of Dynamic Fluorescence Image Data. *Methods in Cell Biology*, 85(08):497–538, 2008.
- [34] Erik Meijering, Oleh Dzyubachyk, Ihor Smal, and Wiggert A. van Cappellen. Tracking in cell and developmental biology. *Seminars in Cell and Developmental Biology*, 20(8):894–902, 2009.
- [35] Ihor Smal, Marco Loog, Wiro Niessen, and Erik Meijering. Quantitative comparison of spot detection methods in fluorescence microscopy. *IEEE Transactions on Medical Imaging*, 29(2):282–301, 2010.
- [36] Erik Meijering, Oleh Dzyubachyk, and Ihor Smal. *Methods for cell and particle tracking*, volume 504. Elsevier Inc., 1 edition, 2012.
- [37] Nicolas Chenuard, Ihor Smal, Fabrice De Chaumont, Martin Maška, Ivo F. Sbalzarini, Yuanhao Gong, Janick Cardinale, Craig Carthel, Stefano Coraluppi, Mark Winter, Andrew R. Cohen, William J. Godinez, Karl Rohr, Yannis Kalaidzidis, Liang Liang, James Duncan, Hongying Shen, Yingke Xu, Klas E.G. Magnusson, Joakim Jaldén, Helen M. Blau, Perrine Paul-Gilloteaux, Philippe Roudot, Charles Kervrann, François Waharte, Jean Yves Tinevez, Spencer L. Shorte, Joost Willemse, Katherine Celler, Gilles P. Van Wezel, Han Wei Dan, Yuh Show Tsai, Carlos Ortiz De Solórzano, Jean Christophe Olivo-Marin, and

- Erik Meijering. Objective comparison of particle tracking methods. *Nature Methods*, 11(3):281–289, 2014.
- [38] Martin Maška, Vladimír Ulman, David Svoboda, Pavel Matula, Petr Matula, Cristina Ederra, Ainhoa Urbiola, Tomás España, Subramanian Venkatesan, Deepak M.W. Balak, Pavel Karas, Tereza Bolcková, Markéta Štreitová, Craig Carthel, Stefano Coraluppi, Nathalie Harder, Karl Rohr, Klas E.G. Magnusson, Joakim Jaldén, Helen M. Blau, Oleh Dzyubachyk, Pavel Křížek, Guy M. Hagen, David Pastor-Escuredo, Daniel Jimenez-Carretero, Maria J. Ledesma-Carbayo, Arrate Muñoz-Barrutia, Erik Meijering, Michal Kozubek, and Carlos Ortiz-De-Solorzano. A benchmark for comparison of cell tracking algorithms. *Bioinformatics*, 30(11):1609–1617, 2014.
- [39] Oliver Hilsenbeck, Michael Schwarzfischer, Stavroula Skylaki, Bernhard Schauberger, Philipp S. Hoppe, Dirk Loeffler, Konstantinos D. Kokkaliaris, Simon Hastreiter, Eleni Skylaki, Adam Filipczyk, Michael Strasser, Felix Buggenthin, Justin S. Feigelman, Jan Krumsiek, Adrianus J.J. Van Den Berg, Max Endele, Martin Etzrodt, Carsten Marr, Fabian J. Theis, and Timm Schroeder. Software tools for single-cell tracking and quantification of cellular and molecular properties. *Nature Biotechnology*, 34(7):703–706, 2016.
- [40] Y. Han, A. M. Alsayed, M. Nobili, J. Zhang, T. C. Lubensky, and A. G. Yodh. Brownian motion of an ellipsoid. *Optics InfoBase Conference Papers*, (October):626–631, 2006.
- [41] F. Boulogne. Custom feature detection and velocity fields: Bubble tracking in 2d foams: <http://soft-matter.github.io/trackpy/v0.4.2/tutorial/custom-feature-detection.html>.

- [42] A. Sauret, F. Boulogne, J. Cappello, E. Dressaire, and H. A. Stone. Damping of liquid sloshing by foams. *Physics of Fluids*, 27(2), 2015, 1411.6542.
- [43] J. Cappello, A. Sauret, F. Boulogne, E. Dressaire, and H. A. Stone. Damping of liquid sloshing by foams: from everyday observations to liquid transport. *Journal of Visualization*, 18(2):269–271, 2015, 1411.2123.
- [44] O. Yang, Y. Peng, Z. Liu, C. Tang, X. Xu, and X. Cheng. Dynamics of ellipsoidal tracers in swimming algal suspensions. *Physical Review E*, 94(4), 2016.
- [45] Jean Yves Tinevez, Nick Perry, Johannes Schindelin, Genevieve M. Hoopes, Gregory D. Reynolds, Emmanuel Laplantine, Sebastian Y. Bednarek, Spencer L. Shorte, and Kevin W. Eliceiri. TrackMate: An open and extensible platform for single-particle tracking. *Methods*, 115:80–90, 2017.
- [46] Jay M. Newby, Alison M. Schaefer, Phoebe T. Lee, M. Gregory Forest, and Samuel K. Lai. Convolutional neural networks automate detection for tracking of submicron-scale particles in 2D and 3D. *Proceedings of the National Academy of Sciences of the United States of America*, 115(36):9026–9031, 2018, 1704.03009.
- [47] Erick Moen, Dylan Bannon, Takamasa Kudo, William Graf, Markus Covert, and David Van Valen. Deep learning for cellular image analysis. *Nature Methods*, 16(12):1233–1246, 2019.
- [48] Dong Qin, Younan Xia, and George M. Whitesides. Soft lithography for micro- and nanoscale patterning. *Nature Protocols*, 5(3):491–502, 2010.
- [49] Jérémie Gachelin, Gastón Miño, Hélène Berthet, Anke Lindner, Annie Rousselet, and Éric Clément. Non-newtonian viscosity of escherichia coli suspensions. *Physical Review Letters*, 110(26):1–5, 2013, 1210.2102.